MATHEMATICAL MODELING AND COMPUTING, Vol. 10, No. 4, pp. 1206–1214 (2023)

Three-dimensional rotating viscous flow past a permeable stretching/shrinking sheet with convective boundary condition

Hafidzuddin M. E. H.[1], Arifin N. M.[2], Nazar R. M.[3], Pop I.[4]

[1] *Centre of Foundation Studies for Agricultural Science, Universiti Putra Malaysia, 43400 UPM Serdang, Selangor, Malaysia*
[2] *Department of Mathematics and Statistics, Faculty of Science, Universiti Putra Malaysia, 43400 UPM Serdang, Selangor, Malaysia*
[3] *Department of Mathematical Sciences, Faculty of Science and Technology, Universiti Kebangsaan Malaysia, 43600 UKM Bangi, Selangor, Malaysia*
[4] *Department of Mathematics, Babes-Bolyai University, 400084 Cluj-Napoca, Romania*

(Received 26 September 2023; Revised 15 November 2023; Accepted 16 November 2023)

The study of three-dimensional rotating boundary layer flow approaching a stretching or shrinking surface under convective boundary conditions is presented in this paper. This study expands the scope of previous researchers' work to encompass broader scenarios, including situations involving mass transfer (suction) on the wall, the Biot number and cases featuring a shrinking surface. It is found that the increase of suction and rotating parameters leads to a noticeable rise in both the local skin friction coefficients and the local Nusselt number, and the solutions to the governing ordinary differential equations exhibit a dual-branch nature, comprising both upper and lower branch solutions, within a specific range of the governing parameters.

Keywords: *three-dimensional flow; rotating flow; convective boundary condition; stretching/shrinking sheet; dual solutions.*

2010 MSC: 35Q35, 80A20, 65L10, 34K10 **DOI:** 10.23939/mmc2023.04.1206

1. Introduction

The rotating viscous boundary layer flow finds significant applications across diverse fields. In atmospheric sciences, it plays a crucial role in comprehending the dynamics of rotating flows within the Earth's atmosphere, including the formation of cyclones and anticyclones. Similarly, in the study of ocean currents, the influence of Earth's rotation on circulation patterns makes the rotating viscous boundary layer flow highly relevant. Some of the important devices include wind turbines, centrifugal compressors and pumps, propellers and machine rotors, cyclones and separators. The principle is utilized in numerous other applications, ranging from aerospace engineering to industrial processes, where the rotation of fluids is harnessed to achieve specific objectives. Wang [1] was among the early pioneers in this field, investigating the two-dimensional stretching of a surface within a rotating fluid. He concluded that at zero or low rotating parameter, the analysis demonstrates a monotonic exponential decay of velocities, while at high rotating parameter, the decay becomes oscillatory. Besides that, it is also found that at high Prandtl numbers, the effect of rotation on heat transfer is relatively small and leads to a minor decrease.

The problem of unsteady flow induced by a shrinking sheet with mass transfer in a rotating fluid is numerically studied by Ali et al. [2]. The Keller-box method was employed to solve the problem, and they concluded that the increase in fluid rotation increases both lateral velocity and velocity profiles. Javed et al. [3] analyzed the effect of rotation on the velocity, boundary layer and skin friction coefficient on the rotating flow of an incompressible viscous fluid over an exponentially stretching

The authors acknowledge the grant from UPM (GP-GPB 9711400).

continuous surface, where they revealed that as the rotation velocity of the frame increases, there is a decrease in the boundary layer thickness and an escalation in the drag force at the surface. This paper is then extended by Rosali et al. [4] by including the mass transfer (suction) on the wall and considering the case of shrinking surface, for which they uncovered that the solutions of the governing ordinary (similarity) differential equations exhibit two branches: upper and lower branch solutions within a particular range of the governing parameters.

Mustafa et al. [5] employed the Tiwari and Das model to investigate the rotational movement and heat transfer of a ferrofluid consisting of magnetite and water over a surface that can deform. They observed that the relationship between the rate of rotation and the rate of stretching has contrasting qualitative impacts on the x- and y-components of velocity. Hayat and Nadeem [6] studied the effects of radiation, heat generation and chemical reaction and the heat transfer characteristics for boundary layer flow of 3D rotating hybrid nanofluid over a linearly stretching sheet. In their paper, it was found that an increase in the rotation parameter leads to an enhancement in the concentration profile. In additional, they also found that the presence of hybridity amplifies both the temperature distribution and the heat transfer rate at the surface. Very recently, a numerical investigation was conducted by Asghar et al. [7] to analyze the dual solutions of rotating stretching/shrinking surfaces by examining how convective boundary conditions, viscous dissipation, thermal radiation, and heat sources/sinks influence the 3-D hybrid nanofluid flow. They found that both solutions are increased in velocity $f'(\eta)$ profile and $g(\eta)$ profile with the increment of positive and negative rotational parameter ω.

A convective boundary condition pertains to the interaction of heat and mass exchange between a solid surface and a flowing fluid (liquid or gas) nearby. This boundary condition is frequently encountered in diverse engineering and natural occurrences, including heat exchangers, cooling systems, and atmospheric flows. Bataller [8] utilized the initial value problem (IVP) technique to obtain numerical solutions for the momentum boundary layers of the Blasius and Sakiadis cases on a horizontal flat plate. Additionally, heat transfer is also considered in the presence of thermal radiation under a convective surface boundary condition. Aziz [9] considered the classical problem of hydrodynamic and thermal boundary layers over a flat plate in a uniform stream of fluid. He showed that a similarity solution becomes feasible when the convective heat transfer from the fluid to the lower surface of the plate is proportional to $x^{-1/2}$. This finding was later extended by Magyari [10] where he conclude that the analytical approach allows for a deep insight in the features of the heat transfer problem under the convective boundary condition.

Akbar et al. [11] explored the numerical simulation of a stable two-dimensional flow at a stagnation point for a nanofluid by considering convective boundary conditions, where they concluded that the variations in the temperature profile and nanoparticle fraction both exhibit an identical trend of increase with respect to the Biot number. Furthermore, the study of nanofluid flow within a rotating frame, where the concurrent impacts of thermal slip and convective boundary conditions are considered by Shafiq et al. [12]. They used the Buongiorno's model, which allows for an exploration of the traits involving Brownian diffusion and thermophoresis, grounded in fundamental principles of symmetry, and numerical solutions are obtained through the employment of the RK45 scheme. They observed an increase in the thermal field due to the elevated augmented Biot number, and as the value of rotation parameter increases, the rate of stretching decreases, leading to a definite impact on the fluid motion. In additional, the flow of a three-dimensional hybrid Cu-Al_2O_3/water nanofluid towards a stretching or shrinking sheet with the inclusion of the effects of velocity slip and convective conditions has been investigated by Khashi'ie et al. [13], where they found that the Biot number has no impact on delaying the boundary layer separation.

In the following year, Hafidzuddin and Alias [14] explored the Navier slip flow phenomenon induced by magnetohydrodynamics (MHD) on a nonlinearly stretching and shrinking sheet in the presence of suction. The findings indicate that suction enhances skin friction, while the slip parameter decreases shear wall stress. Additionally, it is established that the stretching sheet has a smaller range of dual solutions compared to the shrinking case. Moreover, Wahid et al. [15] conducted a numerical investigation into the impact of convective boundary conditions and heat radiation on the flow of

magnetic nanofluids (MNFs) through a permeable moving plate, where they examined increased levels of thermal radiation and Biot number to analyze the heat transfer performance of magnetic nanofluids (MNFs), and determined that higher values of these parameters effectively enhance the heat transfer rate.

Recently, Raju et al. [16] considered the unsteady and incompressible magnetohydrodynamic rotating free convection flow of viscoelastic fluid with simultaneous heat and mass transfer near an infinite vertical oscillating porous plate under the influence of uniform transverse magnetic field and taking Hall current into account. They concluded that the resulting velocity strengthens and encounters deceleration within the flow field as the radiation parameters increase. Conversely, the secondary velocity component rises as the rotation parameters increase.

This article extends the study done in [2] by presenting an investigation into the rotating flow approaching a stretching or shrinking surface under convective boundary conditions. The nonlinear equations for momentum and energy in the form of PDE are reduced to ODE through the application of similarity transformations, which then solved using the `bvp4c` solver in Matlab program. The existence of dual solutions for a certain range of governing parameters are shown graphically. Also, the influence of physical governing parameters on the skin friction coefficient, the local Nusselt number, as well as the velocity and temperature profiles are shown graphically and discussed thoroughly.

2. Problem formulation

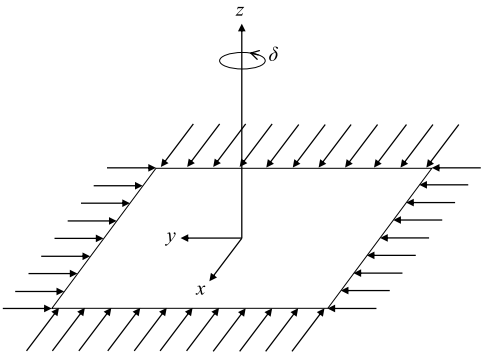

Fig. 1. Physical model and coordinate system for the shrinking surface.

Consider the three-dimensional flow past a stretching/shrinking surface in a rotating fluid, as illustrated in Figure 1. The fluid motion is in three-dimensional due to the Coriolis force [1]. Let (u, v, w) be the velocity components in (x, y, z) direction of the Cartesian axes, respectively, with the axes rotating at an angular velocity δ in the z-direction. The velocities of the sheet along x- and y-directions are u and v, respectively. With these assumptions, the governing Navier–Stokes equations can be defined as [2]:

$$\frac{\partial u}{\partial x} + \frac{\partial v}{\partial y} + \frac{\partial w}{\partial z} = 0, \tag{1}$$

$$u\frac{\partial u}{\partial x} + v\frac{\partial u}{\partial y} + w\frac{\partial u}{\partial z} - 2\delta v = \nu\nabla^2 u, \tag{2}$$

$$u\frac{\partial v}{\partial x} + v\frac{\partial v}{\partial y} + w\frac{\partial v}{\partial z} + 2\delta u = \nu\nabla^2 v, \tag{3}$$

$$u\frac{\partial T}{\partial x} + v\frac{\partial T}{\partial y} + w\frac{\partial T}{\partial z} = \frac{k}{\rho C_p}\nabla^2 T, \tag{4}$$

where ν is the kinematic viscosity, T is the temperature, k is the thermal conductivity, ρ is the fluid density, C_p is the specific heat at the constant pressure, and ∇^2 denotes the three-dimensional Laplacian. Furthermore, it is postulated that convection from a heated fluid at a constant temperature T_f, with a heat transfer coefficient h_f, impacts the lower surface of the sheet. Simultaneously, the temperature at the distant field is denoted as T_∞. The surface $(z = 0)$ is assumed to stretch/shrink in both x- and y-directions such that the boundary conditions are

$$\begin{aligned} &u = \lambda a x, \quad v = 0, \quad w = w_w, \quad -k\frac{\partial T}{\partial z} = h_f(T_f - T) \quad \text{at } z = 0, \\ &u \to 0, \quad v \to 0, \quad w \to 0, \quad T \to T_\infty \quad \text{as } z \to \infty. \end{aligned} \tag{5}$$

In a above-mentioned expressions, λ denotes the stretching ($\lambda > 0$) or shrinking ($\lambda < 0$) parameter, a is a positive constant, and w_w is the constant mass velocity with $w_w(x,t) < 0$ for suction and $w_w(x,t) > 0$ for injection or withdrawal of the fluid.

Following [17], we now introduce the following similarity variables

$$u = axf'(\eta), \quad v = axg(\eta), \quad w = -\sqrt{a\nu}f(\eta), \quad \theta(\eta) = \frac{T - T_\infty}{T_f - T_\infty}, \quad \eta = \sqrt{\frac{a}{\nu}}z, \tag{6}$$

where primes denote the differentiation with respect to η. Using (6), Eq. (1) is satisfied, while Eqs. (2)–(4) are reduced to the following ordinary differential equations

$$f''' + ff'' - f'^2 + 2\alpha g = 0, \tag{7}$$

$$g'' - f'g + fg' - 2\alpha f' = 0, \tag{8}$$

$$\frac{1}{\mathrm{Pr}}\theta'' + f\theta' = 0, \tag{9}$$

subject to the boundary conditions

$$\begin{aligned} &f(0) = s, \quad f'(0) = \lambda, \quad g(0) = 0, \quad \theta'(0) = -\mathrm{Bi}\,(1 - \theta(0)), \\ &f'(\eta) \to 0, \quad g(\eta) \to 0, \quad \theta'(0) \to 0 \quad \text{as } \eta \to \infty. \end{aligned} \tag{10}$$

Here $\alpha = \frac{\delta}{a}$ represents the nondimensional rotating parameter, $\mathrm{Pr} = \frac{\nu}{\kappa}$ is the Prandtl number, $s = -\frac{w_w}{\sqrt{a\nu}}$ is the constant mass flux parameter with $s < 0$ for injection and $s > 0$ for suction, and $\mathrm{Bi} = \sqrt{\frac{\nu}{a}}\frac{h_f}{k}$ represents the Biot number.

The physical quantities of practical interest are the local skin friction coefficients C_{fx}, C_{fy} and the local Nusselt number Nu_x, which are denoted as

$$C_{fx} = \frac{\nu}{(ax)^2}\left(\frac{\partial u}{\partial z}\right)_{z=0}, \quad C_{fy} = \frac{\nu}{(ax)^2}\left(\frac{\partial v}{\partial z}\right)_{z=0}, \quad Nu_x = \frac{x}{T_w - T_\infty}\left(-\frac{\partial T}{\partial z}\right)_{z=0} \tag{11}$$

Using Eqs. (6), (11) becomes

$$\mathrm{Re}_x^{1/2}C_{fx} = f''(0), \quad \mathrm{Re}_y^{1/2}C_{fy} = g'(0), \quad \mathrm{Re}_x^{-1/2}Nu_x = -\theta(0),$$

where $\mathrm{Re}_x = ax^2/\nu$ and $\mathrm{Re}_y = ax^2/\nu$ are the local Reynolds number.

3. Results and discussion

The similarity solutions are derived through the utilization of the `bvp4c` solver to solve the nonlinear ordinary differential equations (7)–(9) while adhering to the specified boundary conditions (10). This solver was developed by Kierzenka and Shampine [18]. To ensure the precision of the numerical outcomes derived in this research, a comparison is made between the reduced skin friction coefficients $f''(0)$ and $g'(0)$ values with those presented in references [5, 7]. The comparisons, as displayed in Table 1, demonstrate remarkable concurrence, instilling us with confidence in the accuracy of the current approach.

Table 1. The comparison findings for $f''(0)$ and $g'(0)$ for several values of α when $s = 0$, $\lambda = 1$, $\mathrm{Pr} = 6.2$.

α	Mustafa et al. [5]		Asghar et al. [7]		Present results	
	$f''(0)$	$g'(0)$	$f''(0)$	$g'(0)$	$f''(0)$	$g'(0)$
0	−1	0	−1	0	−1	0
0.5	−1.13838	−0.51276	−1.138374	−0.512760	−1.138374	−0.512760
1.0	−1.32503	−0.83709	−1.325028	−0.837098	−1.325028	−0.837098
1.5	–	–	−1.496403	−1.082978	−1.496403	−1.082978
2.0	−1.65235	−1.28726	−1.652352	−1.287258	−1.652352	−1.287258
2.5	–	–	−1.795728	−1.465217	−1.795728	−1.465217
3.0	–	–	−1.928931	−1.624735	−1.928931	−1.624735
4.0	–	–	−2.171593	−1.905392	−2.171593	−1.905393
5.0	–	–	−2.390139	−2.150526	−2.390140	−2.150527

Figures 2–8 indicate the existence of dual solutions across a defined range of the stretching/shrinking parameter λ and the mass flux parameter s. By utilizing varying initial approximations for the unknown values of $f''(0)$, $g'(0)$ and $-\theta'(0)$, two separate solutions (first and second) are attained. These solutions are visually represented using solid and dashed lines, respectively. When λ and s reach specific values, such as $\lambda = \lambda_c$ and $s = s_c$ – where λ_c and s_c stand for the critical values of λ and s, respectively – only a singular unique solution emerges. On the other hand, in cases where $\lambda < \lambda_c$ and $s < s_c$, no solution exists. This results in the boundary layer detaching from the surface and renders solutions based on boundary-layer approximations impractical. It is our anticipation that the first solution remains stable and possesses a higher degree of physical relevance, in contrast to the second solution [19–21].

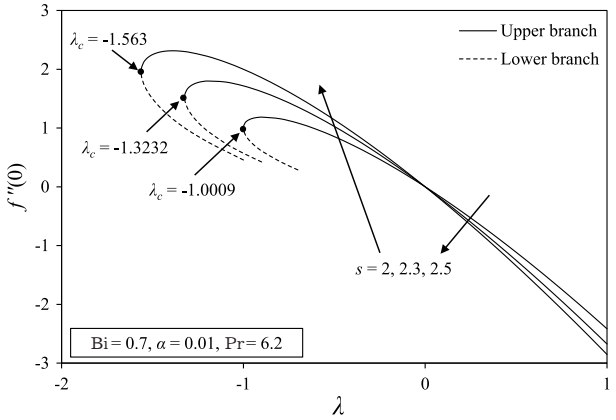

Fig. 2. Variations of $f''(0)$ versus λ with different s.

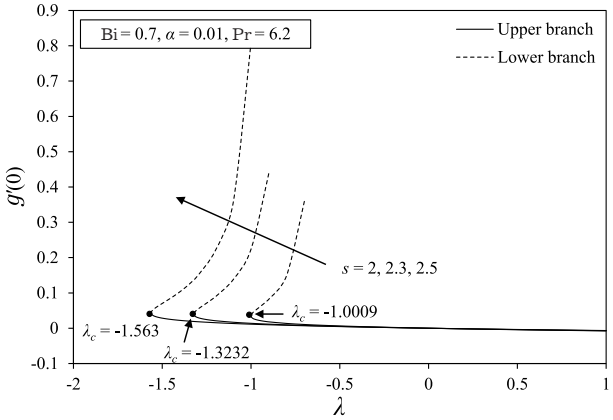

Fig. 3. Variations of $g'(0)$ versus λ with different s.

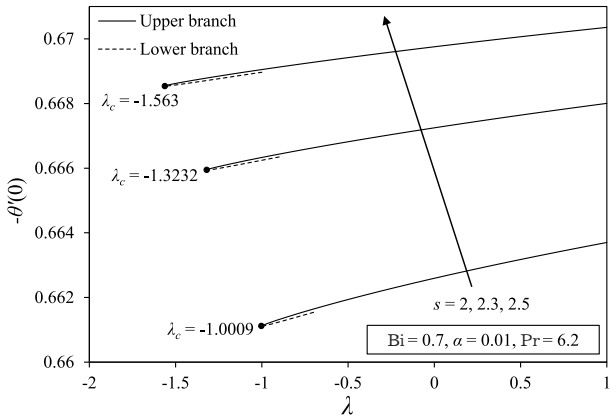

Fig. 4. Variations of $-\theta'(0)$ versus λ with different s.

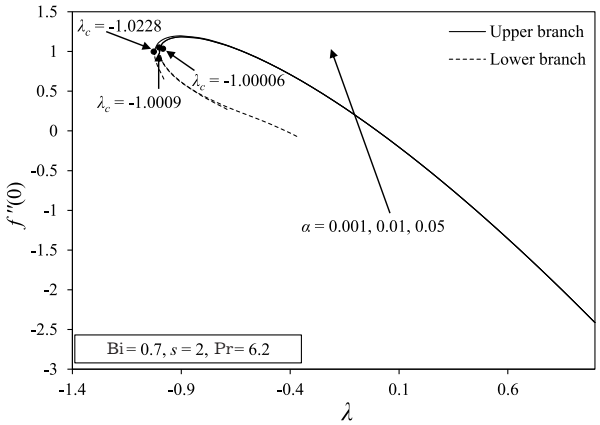

Fig. 5. Variations of $f''(0)$ versus λ with different α.

Figures 2–4 display the influence of an increasing mass flux parameter s against the shrinking parameter λ on the local skin friction coefficients $f''(0)$, $g'(0)$ and the local Nusselt number $-\theta'(0)$ when Bi = 0.7, $\alpha = 0.01$ and Pr = 6.2. It is shown from the figures that the values of $f''(0)$, $g'(0)$ and $-\theta'(0)$ are increasing with the increase of s. Furthermore, it is observed that the second solutions exist when $\lambda < 0$ near the critical values. It is also important to note that as the value of s increases, the magnitudes of $|\lambda_c|$ also increase. Suction diminishes the fluid velocity close to the surface by drawing fluid away. This decline in velocity can result in a more pronounced velocity gradient within the boundary layer. The shear stress at the surface is directly linked to this velocity gradient, indicating that an increased gradient leads to heightened shear stress and subsequently greater skin friction. Furthermore, the reduction in the boundary layer reduces the thermal resistance at the fluid-solid interface, resulting in more efficient heat transfer and a higher local Nusselt number, as shown in Figure 4. This also suggests that a greater amount of suction is necessary to guarantee the existence of a solution on a shrinking sheet, which corresponds with the finding established by Miklavcic and Wang [22].

The variation in the local skin friction coefficients $f''(0)$, $g'(0)$, and the local Nusselt number $-\theta'(0)$ due to the increasing rotational parameter α relative to the shrinking parameter λ is depicted in Figures 5–7. These representations consider the conditions Bi = 0.7, $s = 2$, and Pr = 6.2. It can also be seen that the boundary layer separation is delayed as the value of α is increasing. Observing the trend, it becomes evident that augmenting the rotational parameter leads to a rise in the local skin friction. This is because rotation generates secondary flow patterns, such as Ekman spirals, because of the Coriolis effect [1]. These secondary flows have the capacity to redistribute momentum and energy within the boundary layer, thereby playing a role in postponing separation. When considering a contracting surface, the secondary flows engendered by rotation facilitate the movement of higher-momentum fluid from the outer boundary layer region toward the surface, thereby adding to the prevention of separation.

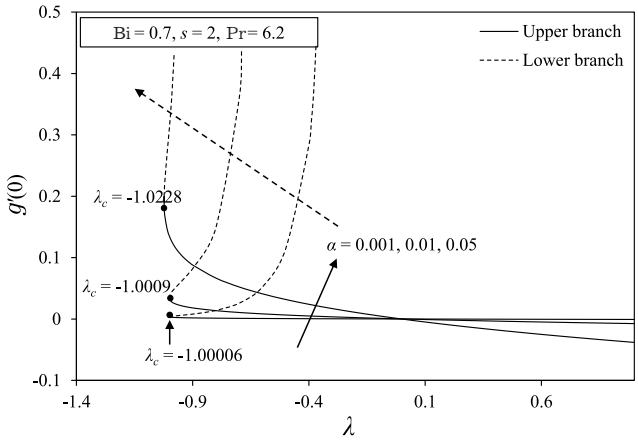

Fig. 6. Variations of $g'(0)$ versus λ with different α.

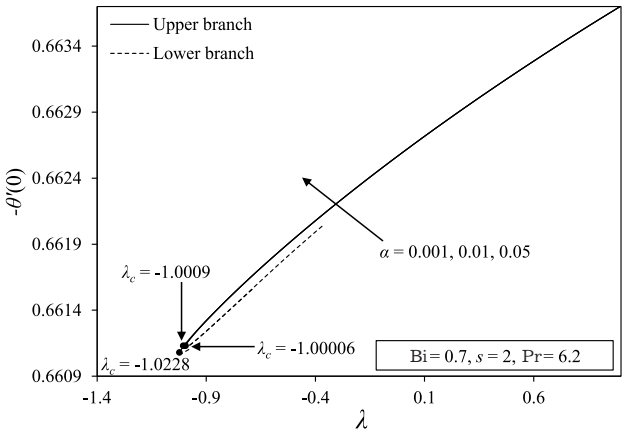

Fig. 7. Variations of $-\theta'(0)$ versus λ with different α.

Conversely, an inverse impact is noticed in relation to the local Nusselt number, as depicted in Figure 7. As previously mentioned, the secondary flow patterns and centrifugal forces induced by rotation enhance the transport of momentum and energy within the boundary layer. This increased transport results in more efficient mixing of fluid near the surface, which in turn reduces the temperature gradient in the boundary layer. A smaller temperature gradient leads to lower convective heat transfer rates, resulting in a decreased local Nusselt number.

There is a noticeable elevation in the surface heat transfer rate with the increase in the Biot number (Bi), as depicted in Figure 8. The connection between the surface heat transfer rate and the Biot number (as described in boundary condition (10)) is straightforward. The convective heating mechanism influences the surface temperature, causing an amplification of the surface heat transfer rate as the Biot number increases. The depicted result also shows that adjustments in the Biot number do not play a role in postponing the separation of the boundary layer. In additional, as the Biot number increases, the thermal boundary layer near the surface becomes thicker, as displayed in Figure 9. Convective heat transfer from the fluid to the solid takes precedence, while heat conduction within the solid has a comparatively reduced effect. Consequently, a more pronounced temperature gradient forms across the solid, resulting in an augmented thickness of the thermal boundary layer within the fluid adjoining the surface.

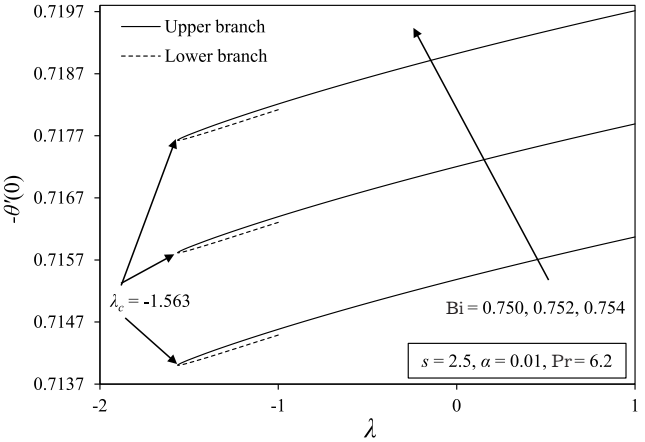

Fig. 8. Variations of $-\theta'(0)$ versus λ with different Bi.

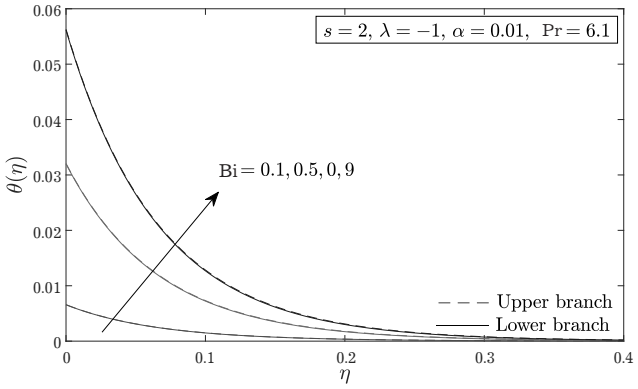

Fig. 9. $\theta(\eta)$ for several values of Bi.

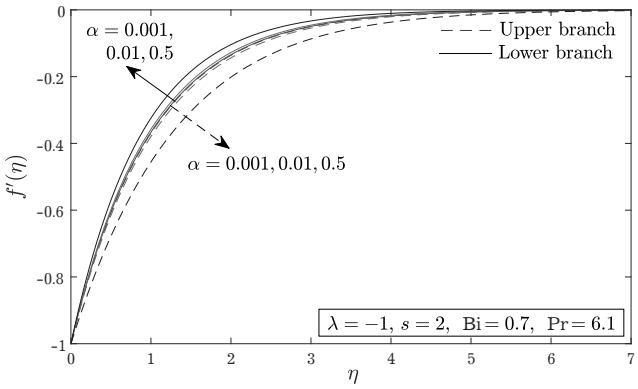

Fig. 10. $f'(\eta)$ for several values of α.

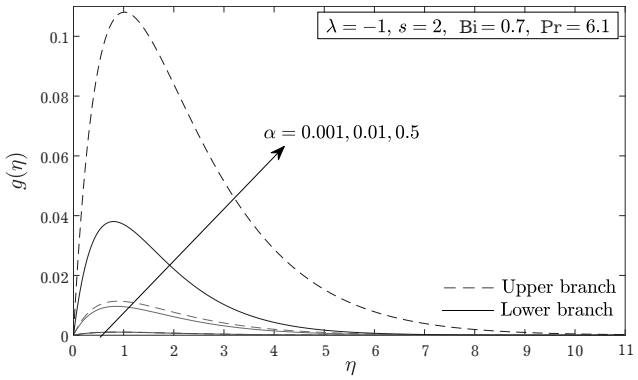

Fig. 11. $g(\eta)$ for several values of α.

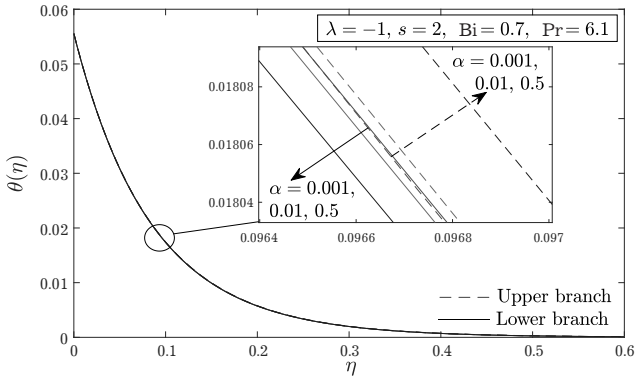

Fig. 12. $\theta(\eta)$ for several values of α.

The figures for velocity profiles $f'(\eta)$, $g(\eta)$ and temperature profiles $\theta(\eta)$ for different rotating parameter α are illustrated in Figures 10, 11 and 12, respectively. These there figures prove that as the rotating parameter increases, it leads to the thinner boundary layer. Following the discussion from the previous paragraph, the secondary flow phenomenon causes the velocity distribution across the boundary layer becomes more uniform, which in turn causing a decrease in the velocity gradient near the surface. Furthermore, rotation has the capability to hinder the expansion of the thermal boundary layer by virtue of the effective mixing prompted by secondary flows. This inhibition additionally plays a role in diminishing the overall thickness of the boundary layer.

4. Conclusions

An investigation into three-dimensional rotating boundary layer flow approaching a stretching or shrinking surface under convective boundary conditions has been carried out. The numerical calculations via `bvp4c` solver in MATLAB revealed a strong concordance between the current findings of the local skin friction coefficients and the outcomes obtained from a prior study concerning a stretching surface under conditions lacking the mass transfer (suction) parameter. Through these numerical calculations, the physically significant values are able to be computed efficiently, including skin friction coefficients, heat transfer rates, velocity and temperature profiles, across a range of governing parameters. These parameters encompass suction, stretching/shrinking, Biot number, Prandtl number, and rotation parameters. To sum up,

— In a defined range of suction and stretching/shrinking parameters, it becomes evident that dual solutions are present.
— With an elevation in the values of suction and rotating parameters, there is an observed increase in both the local skin friction coefficients and the local Nusselt number.
— The local Nusselt number shows an upward trend as the Biot number increases.

— The increment of the rotating parameter leads to a decrease in the boundary layer thickness, whereas an opposite trend is noticed for the thermal boundary layer thickness as the Biot number increases.

Acknowledgments

The authors wish to thank the very competent reviewers for the very good comments and suggestions. The financial supports received from the Universiti Putra Malaysia in a form of research grant (Vot number: GP-GPB 9711400) is gratefully acknowledged.

[1] Wang C. Y. Stretching a surface in a rotating fluid. Zeitschrift für angewandte Mathematik und Physik ZAMP. **39** (2), 177–185 (1988).

[2] Ali F. M., Nazar R., Arifin N. M., Pop I. Unsteady shrinking sheet with mass transfer in a rotating fluid. International Journal for Numerical Methods in Fluids. **66** (11), 1465–1474 (2011).

[3] Javed T., Sajid M., Abbas Z., Ali N. Non-similar solution for rotating flow over an exponentially stretching surface. International Journal of Numerical Methods for Heat & Fluid Flow. **21** (7), 903–908 (2011).

[4] Rosali H., Ishak A., Nazar R., Pop I. Rotating flow over an exponentially shrinking sheet with suction. Journal of Molecular Liquids. **211**, 965–969 (2015).

[5] Mustafa M., Mushtaq A., Hayat T., Alsaedi A. Rotating Flow of Magnetite-Water Nanofluid over a Stretching Surface Inspired by Non-Linear Thermal Radiation. PLOS ONE. **11** (2), e0149304 (2016).

[6] Hayat T., Nadeem S. Heat transfer enhancement with Ag-CuO/water hybrid nanofluid. Results in Physics. **7**, 2317–2324 (2017).

[7] Asghar A., Vrinceanu N., Yuan Ying T., Ali Lund L., Shah Z., Tirth V. Dual solutions of convective rotating flow of three-dimensional hybrid nanofluid across the linear stretching/shrinking sheet. Alexandria Engineering Journal. **75**, 297–312 (2023).

[8] Bataller R. C. Radiation effects for the Blasius and Sakiadis flows with a convective surface boundary condition. Applied Mathematics and Computation. **206** (12), 832–840 (2008).

[9] Aziz A. A similarity solution for laminar thermal boundary layer over a flat plate with a convective surface boundary condition. Communications in Nonlinear Science and Numerical Simulation. **14** (4), 1064–1068 (2009).

[10] Magyari E. Comment on "A similarity solution for laminar thermal boundary layer over a flat plate with a convective surface boundary condition" by A. Aziz, Comm. Nonlinear Sci. Numer. Simul. **14**, 1064-8 (2009). Communications in Nonlinear Science and Numerical Simulation. **16** (1), 599–601 (2011).

[11] Akbar N. S., Nadeem S., Haq R. U., Khan Z. Radiation effects on MHD stagnation point flow of nano fluid towards a stretching surface with convective boundary condition. Chinese Journal of Aeronautics. **26** (6), 1389–1397 (2013).

[12] Shafiq A., Rasool G., Khalique C. Significance of Thermal Slip and Convective Boundary Conditions in Three Dimensional Rotating Darcy-Forchheimer Nanofluid Flow. Symmetry. **12** (5), 741 (2020).

[13] Khashi'ie N. S., Arifin N. M., Pop I., Nazar R., Hafidzuddin E. H., Wahi N. Three-Dimensional Hybrid Nanofluid Flow and Heat Transfer past a Permeable Stretching/Shrinking Sheet with Velocity Slip and Convective Condition. Chinese Journal of Physics. **66**, 157–171 (2020).

[14] Hafidzuddin M. E. H., Alias N. S. Effect of suction and MHD induced Navier slip flow due to a non-linear stretching/shrinking sheet. Mathematical Modeling and Computing. **9** (1), 83–91 (2022).

[15] Wahid N. S, Arifin N. M., Khashi'ie N. S., Pop I., Bachok N., Hafidzuddin M. E. H. Radiative flow of magnetic nanofluids over a moving surface with convective boundary condition. Mathematical Modeling and Computing. **9** (4), 791–804 (2022).

[16] Raju G., Hari Babu B., Rama Mohan Reddy L., Varma S. MHD convective rotating flow of viscoelastic fluid past an infinite vertical oscillating porous plate with Hall effects. Heat Transfer. **52**, 2277–2294 (2023).

[17] Surma Devi C., Takhar H., Nath G. Unsteady, three-dimensional, boundary-layer flow due to a stretching surface. International Journal of Heat and Mass Transfer. **29** (12), 1996–1999 (1986).

[18] Kierzenka J., Shampine L. A BVP Solver that Controls Residual and Error. Journal of Numerical Analysis, Industrial and Applied Mathematics. **3** (1–2), 27–41 (2008).

[19] Merkin J. On dual solutions occurring in mixed convection in a porous medium. Journal of Engineering Mathematics. **20**, 171–179 (1986).

[20] Weidman P., Kubitschek D., Davis A. The effect of transpiration on self-similar boundary layer flow over moving surfaces. International Journal of Engineering Science. **44** (11–12), 730–737 (2006).

[21] Rosca A. V., Pop I. Flow and heat transfer over a vertical permeable stretching/shrinking sheet with a second order slip. International Journal of Heat and Mass Transfer. **60**, 355–364 (2013).

[22] Miklavčič M., Wang C. Viscous flow due to a shrinking sheet. Quarterly of Applied Mathematics. **64** (2), 283–290 (2006).

Тривимірне обертове в'язке обтікання проникного листа, що розтягується/стискається, з конвективною граничною умовою

Хафідзуддін М. Е. Х.[1], Аріфін Н. М.[2], Назар Р. М.[3], Поп І.[4]

[1]*Центр фундаментальних досліджень сільськогосподарської науки, Університет Путра Малайзія, 43400 UPM Серданг, Селангор, Малайзія*
[2]*Кафедра математики і статистики, факультет природничих наук, Університет Путра Малайзія, 43400 UPM Серданг, Селангор, Малайзія*
[3]*Кафедра математичних наук, факультет науки і техніки, Університет Кебангсан Малайзії, 43600 UKM Бангі, Селангор, Малайзія*
[4]*Кафедра математики, Університет Бабеш-Бойяї, 400084 Клуж-Напока, Румунія*

У цій статті представлено дослідження тривимірного обертового потоку граничного шару, яка наближається до поверхні, що розтягується або стискається, за конвективних граничних умов. Це дослідження розширює сферу роботи попередніх дослідників, щоб охопити ширші сценарії, включаючи ситуації, які пов'язані з перенесенням маси (всмоктуванням) на стінці, числом Біо та випадками стягування поверхні. Виявлено, що збільшення параметрів всмоктування та обертання призводить до помітного зростання як локальних коефіцієнтів поверхневого тертя, так і локального числа Нуссельта, а розв'язки основних звичайних диференціальних рівнянь мають подвійну природу, що включає як верхню, так і нижню гілки розв'язку в межах певного діапазону визначальних параметрів.

Ключові слова: *тривимірний потік; обертовий потік; конвективна гранична умова; лист, що розтягується/стискається; подвійні рішення.*